A peer-reviewed version of this preprint was published in PeerJ on 5 June 2018.

Asthana V, Tang Y, Ferguson A, Bugga P, Asthana A, Evans ER, Chen AL, Stern BS, Drezek RA. 2018. An inexpensive, customizable microscopy system for the automated quantification and characterization of multiple adherent cell types. PeerJ 6:e4937
https://doi.org/10.7717/peerj.4937

A customizable microscopy system for the automated quantification and characterization of multiple adherent cell types: an alternative to flow cytometry

Vishwaratn Asthana [Corresp., 1], **Yuqi Tang** [1], **Adam Ferguson** [1], **Pallavi Bugga** [1], **Anantratn Asthana** [2], **Emily R Evans** [1], **Allen L Chen** [1], **Brett S Stern** [1], **Rebekah A Drezek** [1]

[1] Department of Bioengineering, Rice University, Houston, Texas, United States

[2] Department of Molecular & Cell Biology, University of California, Berkeley, Berkeley, California, United States

Corresponding Author: Vishwaratn Asthana
Email address: va14@rice.edu

Cell quantification assays are essential components of most biological and clinical labs. However, many currently available quantification assays, including flow cytometry and commercial cell counting systems, suffer from unique drawbacks that limit their overall efficacy. In order to address the shortcomings of traditional quantification assays, we have designed a robust, low-cost, automated optical cell cytometer that quantifies individual cells in a multiwell plate using tools readily available in most labs. Plating and subsequent quantification of various dilution series using the automated optical cytometer demonstrates the single-cell sensitivity, near-perfect R^2 accuracy, and greater than 5-log dynamic range of our system. Further, the optical cytometer is capable of obtaining absolute counts of multiple cell types in one well as part of a co-culture setup. To demonstrate this ability, we recreated an experiment that assesses the tumoricidal properties of primed macrophages on co-cultured tumor cells as a proof-of-principle test. The results of the experiment reveal that primed macrophages display enhanced cytotoxicity towards tumor cells while simultaneously losing the ability to proliferate, an example of a dynamic interplay between two cell populations that our optical cytometer is successfully able to elucidate.

A Customizable Microscopy System for the Automated Quantification and Characterization of Multiple Adherent Cell Types: an Alternative to Flow Cytometry

Vishwaratn Asthana[1*], Yuqi Tang[1¶], Adam Ferguson[1¶], Pallavi Bugga[1], Anantratn Asthana[2], Emily R. Evans[1], Allen L. Chen[1], Brett S. Stern[1], Rebekah A. Drezek[1]

[1] Department of Bioengineering, Rice University, Houston, Texas, United States of America, [2] Berkeley University, Berkeley, California, United States of America

[*] Corresponding author

E-mail: vishwaratn.asthana@rice.edu (VA)

[¶] These authors contributed equally to this work.

Cell quantification assays are essential components of most biological and clinical labs. However, many currently available quantification assays, including flow cytometry and commercial cell counting systems, suffer from unique drawbacks that limit their overall efficacy. In order to address the shortcomings of traditional quantification assays, we have designed a robust, low-cost, automated optical cell cytometer that quantifies individual cells in a multiwell plate using tools readily available in most labs. Plating and subsequent quantification of various dilution series using the automated optical cytometer demonstrates the single-cell sensitivity, near-perfect R^2 accuracy, and greater than 5-log dynamic range of our system. Further, the optical cytometer is capable of obtaining absolute counts of multiple cell types in one well as part of a co-culture setup. To demonstrate this ability, we recreated an experiment that assesses the tumoricidal properties of primed macrophages on co-cultured tumor cells as a proof-of-principle test. The results of the experiment reveal that primed macrophages display enhanced cytotoxicity towards tumor cells while simultaneously losing the ability to proliferate, an example of a dynamic interplay between two cell populations that our optical cytometer is successfully able to elucidate.

PeerJ Preprints | https://doi.org/10.7287/peerj.preprints.26584v1 | CC BY 4.0 Open Access | rec: 1 Mar 2018, publ: 1 Mar 2018

Introduction

Cell quantification assays are essential components of most biological labs, and are used for a variety of applications, including cytotoxicity, viability, and proliferative studies. Though these assays have improved significantly since the advent of hemocytometers, they still suffer from a number of unique limitations. Current cell quantification assays can be divided into two major classes: metabolic and cell counting. Metabolic assays, though originally designed to assess cell viability, are often used to indirectly assess cell number. These assays, like MTT or alamarBlue, are relatively easy to perform, and can provide additional information on cell health that a counting assay may not. However, they are not ideal for certain experimental setups, as they have a limited dynamic range and are prone to confounding interference in the presence of certain chemicals (Chakrabarti et al. 2000; Doak et al. 2009; Hamid et al. 2004; Ulukaya et al. 2004; Vistica et al. 1991). These assays also do not always align well with the DNA content of the cell—a parameter that correlates strongly with cell number—limiting the cell quantification potential of these assays (Quent et al. 2010). Cell counting assays on the other hand, though generally more manually intensive, are more representative of actual cell counts than metabolic-based proxy assays (Chan et al. 2013). Flow cytometry, often considered the gold standard for cell counting and analysis, is an especially powerful technique for quantifying individual cells, and is one of the few modalities capable of identifying cell population counts in both a mono-culture and co-culture setup (Gedye et al. 2014; Gerashchenko 2008; Gerashchenko & Howell 2013).

Co-culture systems are fundamental to studying any kind of cell-to-cell interaction. Many areas of research could benefit immensely from co-culture setups—including biomaterials, immunology, and cancer biology—if better characterization and quantification methods were

available for these studies (Bidarra et al. 2011; Miki et al. 2012). Most approaches to co-culture are restrictive, and often require that plated cells be physically separated via a transwell insert or microfluidic chamber that only permits the exchange of media (Arrigoni et al. 2016; Goers et al. 2014; Katt et al. 2016). Yet physical contact has been shown to be important for studying the interactions of many cell types in a variety of physiological contexts (Cruickshank et al. 2004; de Goer de Herve et al. 2010; Holt et al. 2010; Suzuki et al. 2004). Most cell populations do not behave independently and a better understanding of the interaction between multiple cell types in a system will help improve our understanding of many physiological phenomena.

Most studies that utilize a true co-culture setup with physical contact rely on flow cytometry to quantify individual cell types. Unfortunately, flow cytometry has several drawbacks that apply not only to co-culture setups but mono-culture setups as well. As a starting point, flow cytometers are fairly sophisticated; as a result, these instruments are generally expensive and often require skilled upkeep (Nasi et al. 2015). Flow cytometry also requires cells to be in suspension—thus the majority of experiments that are conducted on adherent cells in multiwell plates require trypsin treatment for cell detachment. Trypsin, however, can damage cells and cleave extracellular markers that may be used for cellular identification or other forms of analysis (Gedye et al. 2014). Additionally, certain cell types are not amenable to trypsin treatment and as a result require manual cell scraping, a process that is prone to human error. Cell scraping can also mechanically damage some cell types, leading to erroneous results with certain assays that are used in combination with flow cytometry: for example, false positives with membrane permeable cell viability assays such as propidium iodide (Batista et al. 2010; Bundscherer et al. 2013). All together, the need to bring adherent cells into suspension makes flow cytometry less than ideal for many types of studies.

An additional limitation unique to co-culture setups is that typical flow cytometry obtains relative counts rather than absolute counts, i.e. each cell type is expressed as a percent of the total sample assayed. This may generate misleading results when comparing counts for multiple cell types between conditions.

To address the shortcomings of the various cell quantification assays, we have put together a relatively simple optical counting setup with tools readily available in most labs (Fig 1). The proposed system uses a standard fluorescent microscope to quantify individual cells on a multiwell plate with superior sensitivity, resolution, and dynamic range. The system utilizes established staining techniques to label cells, and subsequently quantifies every cell in the entire experimental space via whole-well imaging, thus precluding the need for trypsinization or cell scraping. The image data is then run through ImageJ for preprocessing and then analyzed in CellProfiler, a free-to-use cell segmentation software, to generate absolute cell counts for every well. In addition, by utilizing a combination of staining techniques, multiple cell types (even those with complex morphologies) can be uniquely identified and absolutely counted, permitting the setup of more complicated co-culture experiments that were not previously feasible, one of the strongest aspects of the proposed system.

It should be noted that other optical counting systems have been developed to address the aforementioned limitations of flow cytometry. However, the optical system we present here still bears a number of advantages over these pre-sold cytometric platforms. First, for labs that already possess a fluorescent microscope, the optical cytometer is a relatively small investment to the overhead cost of buying a prebuilt optical counting system or flow cytometer. Further, unlike most commercial counting systems, the optical cytometer discussed here is flexible in the assays and cell types that can potentially be analyzed, and highly customizable in both setup and

analysis, permitting the extraction of more relevant and robust information per experiment. In this way, biological workflow is not limited by the vendor-specific restrictions of pre-built systems, but rather expanded to include all functionalities of standard fluorescent microscopes.

Many image cytometers currently on the market also exhibit a smaller dynamic range and reduced sensitivity compared to the system we present here. Lastly, most commercial cytometric platforms are not able to discriminate multiple unique cell populations, with potentially complex morphologies, within a single well. This is largely due to the inability of most commercial cytometers to accurately segment non-spherical morphologies, thus restricting their applicability for most co-culture setups. A more in depth comparison of our optical cytometer to commercially available systems, including in cost, can be found in the discussion as well as supplementary section (Text S1).

Materials and Methods

Cell Culture and Plating

JC CRL 2116 mouse adenocarcinoma cells were obtained from ATCC (American Type Culture Collection; Manassas, Virginia) and maintained in Dulbecco's Modified Eagle Medium (DMEM) supplemented with 10% Fetal Bovine Serum (FBS) and 1% penicillin/streptomycin. J774.A1 mouse macrophages were obtained from ATCC and maintained in Roswell Park Memorial Institute Medium (RPMI), supplemented with 10% Fetal Bovine Serum (FBS) and 1% penicillin/streptomycin. Both cells were grown at 37°C in 5% CO_2.

For plating, cells were trypsinized (JC CRL 2216 cells) or scraped (J774.A1 cells) from their flasks and quantified manually using a bright-line hemocytometer (Sigma-Aldrich; St. Louis, Missouri). Due to the variability present in counts obtained using a hemocytometer, established values were primarily used to determine the approximate concentration of the

primary stock from which precise subsequent dilutions were performed. Dilution series were generated by pulling cells from the previous stock and diluting in fresh media. Triplicates of each dilution were then plated on either a 48- or 12-well Corning Costar flat bottom cell culture plate (Thermo Fisher Scientific; Waltham, Massachusetts) and left overnight to attach to the plate surface.

Co-Culture Experiments

J774.A1 cells were seeded at 2.5×10^4 cells/well in RPMI media in a 48-well plate. Immediately following seeding, cells were exposed either to 1 μg/mL of lipopolysaccharide (LPS) (Sigma-Aldrich; St. Louis, Missouri), 0.1 μg/mL of mouse interferon gamma (IFNγ) (BioLegend; San Diego, California), both 1 μg/mL of LPS and 0.1 μg/mL of IFNγ, or neither. After a 24-hour incubation, the wells were washed twice with Phosphate Buffered Saline (PBS). JC CRL 2116 cells were then added at 1×10^4 cells/well in RPMI media to every well. Cells were processed and imaged after 24 hours.

Cell Staining

For assays requiring only a nuclear stain, cell processing was performed immediately prior to imaging. After firm cell adhesion, media was removed from the wells by inverting the plate and cells were fixed for 15 minutes in BD Cytofix (BD Biosciences; San Jose, California). Fixative was removed by washing the plate twice with Hank's Balanced Salt Solution (HBSS). Cells were then stained for 5 minutes in a 2.5 μg/mL DAPI stain solution (Thermo Fisher Scientific; Waltham, Massachusetts). The plate was again washed twice with HBSS and finally resuspended in HBSS for imaging.

Experiments involving multiple stains, including nuclear, cytoplasmic, and surface/antibody stains, required a slightly different protocol. Using the immune co-culture

experiment as an example, JC CRL 2116 cells were stained in their cell culture flask with 20 µM of Vybrant CFDA SE (Invitrogen; Carlsbad, California) the day prior to plating using the recommended protocol. After completion of the experiment and immediately prior to imaging, media was removed from the wells by inverting the plate, and the plate was subsequently blocked with a 1% bovine serum albumin (BSA) (Sigma-Aldrich; St. Louis, Missouri) solution in HBSS for 15 minutes. HBSS supplemented with calcium was found to help prevent cell detachment prior to cell fixation. Cells were then incubated with a 5 µg/mL PE anti-mouse CD11b antibody (BioLegend; San Diego, California) diluted in 1% BSA HBSS for 1 hour to stain the J774.A1 cells. After incubation, the antibody solution was removed by inverting the plate after which the wells were washed twice with 1% BSA HBSS. The cells were then fixed for 20 minutes in BD Cytofix. Fixative was removed by washing the plate twice with HBSS. Cells were then stained for 5 minutes in a 2.5 µg/mL DAPI stain solution. The plate was again washed twice with HBSS and finally resuspended in HBSS for imaging.

Acquiring Whole-Well Images

All imaging was performed on a Nikon Eclipse Ti-E inverted fluorescent microscope with motorized x, y, and z stage (Nikon Instruments Inc.; Melville, New York). Images were captured using a NAMC 10x objective and Andor Zyla 4.2 sCMOS camera (Andor Technology; Belfast, Northern Ireland). DAPI/Hoechst (excitation: 360/40, emission: 460/50, dichroic mirror: 400), GFP (Ex: 470/40, Em: 525/50, DM: 495), and Texas Red (Ex: 560/55, Em: 645/75, DM: 595) filter cubes (Nikon Instruments Inc.; Melville, New York) were used to image cells stained with DAPI, Vybrant CFDA SE, and PE anti-mouse CD11b antibody respectively. Using the associated Nikon software, NIS-Elements, an automated macro was set up for whole-well acquisition. First, an x-y coordinate list demarcating the center of every well was generated by

manually determining the center of the first and last well of the plate and dividing these values by the number of rows and columns. The coordinate list will vary based on the type of multiwell plate but only needs to be generated once. Using a 10× objective and 1,600×1,600 pixel region of interest (ROI), 10×10 images for a 48-well plate and 19×19 images for a 12-well plate were tiled together to create a whole-well image. The center of each well serves as the origin point of the tiled images as well as the autofocus point.

Processing Whole-Well Images

Images were preprocessed using ImageJ (National Institute of Health; Bethesda, Maryland). The ring of autofluorescence around the well edges was removed using the *Subtract Background* function with a rolling ball radius of 50 pixels. Fluorescent channels that were too faint for analysis were occasionally made brighter using the *Enhance Contrast* function. If images were stitched during image acquisition they were subsequently cropped into 100 smaller images using the *Montage to Stack* function at which point they were transferred to CellProfiler (Broad Institute; Cambridge, Massachusetts) for segmentation. ImageJ macros (Macro S1) and CellProfiler codes (CellProfiler Code S1, and CellProfiler Code S2) are provided as supplementary files. A more detailed explanation of relevant ImageJ and CellProfiler functions can be found in the supplementary section (Text S1).

Results

Accuracy of Nuclear Quantification in Conjunction with Whole-Well Imaging

Many studies take representative or random images that represent only a small portion of the entire well to make a claim about differences in cell count/viability between conditions. Instead of manually acquiring a series of random or representative images, which is both tedious and potentially inaccurate, it is possible—using a fluorescent microscope with a motorized x, y,

and z stage—to automate capture of the whole well using movement in the x- and y-plane to image the well and movement in the z-plane to autofocus (Fig 2).

To count individual cells, wells were stained with a DAPI nuclear stain. Nuclei are often roundly shaped and spaced from adjacent nuclei by the cell cytoplasm and membrane, making segmentation relatively straightforward. In addition, there is usually one nucleus per cell, making nuclear segmentation ideal for cell counting. To demonstrate the power of nuclear counting and whole-well imaging, a linear dilution series of JC CRL 2116 mouse adenocarcinoma cells going from 10,000 cells/well all the way down to 1,000 cells/well was plated; an experiment spanning one order of magnitude. Three linear curves were then generated from five random images, a box crop of the whole-well image, or the whole-well image itself, and used to determine cell count (Fig 3). Accuracy improves significantly as the percentage of the experimental space being assayed increases, with whole-well imaging displaying a near-perfect R^2 and minimal error between replicates.

Establishing Dynamic Range and Sensitivity

The optical cell cytometer obtains accurate counts by counting individual cells. In theory it should be able to count anywhere from one cell to the confluency limit of the well plate the experiment is conducted in with single-cell precision. To demonstrate the dynamic range of the system, half-log dilutions of JC CRL 2116 cells going from 100,000 cells/well all the way down to 100 cells/well were plated in a 12-well plate; an experiment spanning three orders of magnitude (Fig 4). The system performs strongly up to the confluency limit of the plate with a dynamic range limited only by the surface area of the multiwell. Even at confluency, nuclei remain sufficiently spaced apart permitting accurate segmentation (Fig S1).

To validate the sensitivity of the system, a linear dilution series starting at 100 cells/well and going down to 1 cell/well was also plated. However it was found that at such low concentrations, it was not feasible to reliably plate the desired number of cells. Accordingly, the cells that were plated were manually counted in the brightfield channel and compared with CellProfiler counts obtained from segmenting nuclei in the DAPI channel (Fig 5). The system demonstrates an extraordinary level of sensitivity and resolution, as it performs robustly even at the single-cell level, with most deviations attributable to human error when manually counting.

Counting Using Surface and Cytoplasmic Stains

In order to count multiple cell types in a co-culture experiment, additional cell stains are required. Cell stains can be grouped into one of three categories: nuclear, surface, and cytoplasmic. Because most nuclear stains non-specifically stain DNA and compromise cell viability, they cannot be used to differentiate cell types. Instead, vital cytoplasmic dyes like Vybrant CFDA SE (Vybrant carboxyfluorescein diacetate succinimidyl ester), or antigen-specific surface stains, such as fluorophore-conjugated antibodies, need to be used.

Surface and cytoplasmic staining alone can be used to differentiate cells, but primary segmentation of these stains is fairly difficult. Factors including inhomogeneous staining, cell contact with neighboring objects, and complex cell morphologies make segmentation less than ideal. One way to overcome this limitation is to use easily identifiable and spatially resolvable nuclei delineated in one fluorescent channel as a seed/primary object to guide detection of the cell border/secondary object outlined in a separate fluorescent channel (Jones et al. 2005; Vincent & Soille 1991). However, when plating more than one cell type, for example in a co-culture setup, this approach alone is insufficient because every nuclei will generate a secondary object regardless of whether there is an associated cell in CellProfiler (Carpenter et al. 2006). To

overcome this limitation, several additional layers of image processing, including mask generation, need to be performed; these are elaborated upon in the discussion section.

To validate the power of this approach as well as the efficacy of cytoplasmic and surface staining, a linear dilution series of J774.A1 cells, a mouse macrophage cell line, was plated going from 10,000 cells/well down to 1,000 cells/well. These cells were stained with Vybrant CFDA SE (cytoplasmic stain) prior to plating, and phycoerythrin (PE)-conjugated anti-CD11b antibodies (surface stain) as well as DAPI (nuclear stain) immediately prior to imaging. The system performs less than ideally when segmenting the cytoplasmic or surface stains alone (Fig S2). When nuclei are used as seeds however, the optical cytometer performs robustly both for cytoplasmic and surface staining (Fig 6).

Quantification of Multiple Adherent Cell Types

To demonstrate the ability of the optical cell cytometer to determine absolute counts of multiple cell types in a single well, we recreated an immunology experiment that was conducted in 1991 as a proof-of-principle test. Novotney, et al. set out to determine the tumoricidal properties of J774.A1 mouse macrophages when primed with lipopolysaccharide (LPS). To do this, the target tumor cell line needed to be radiolabeled with ^{51}Cr then co-cultured with primed J774.A1 macrophages. The extent of tumor killing was determined by measuring the increase in radioactivity of the supernatant due to tumor cell death and detachment (Novotney et al. 1991).

To recreate this experiment, JC CRL 2116 tumor cells were labeled with Vybrant CFDA SE in their cell culture flask 24 hours prior to plating. J774.A1 macrophages were plated first and were either left unprimed or primed with either LPS, interferon gamma (IFNγ)—a known macrophage activator, or both (Schoenborn & Wilson 2007). After a 24-hour incubation, LPS and IFNγ were removed from the wells and the previously stained JC CRL 2216 cells were

added. After another 24-hour incubation, the wells were stained with a PE-conjugated anti-CD11b targeting antibody to uniquely label the J774.A1 macrophages, as well as DAPI to stain all nuclei.

The results of the test reveal an interesting relationship between macrophage activation and tumoricidal activity. The more strongly primed the macrophages, the more pronounced the tumoricidal response; however, strongly primed macrophages also lose the ability to proliferate, indicated by a sharp drop in macrophage count (Fig 7a). Absolute counts of both cell populations show that erroneous results would have been obtained by any setup that looks at relative counts (Fig 7b). Cytometric analysis reveals that primed J774.A1 macrophages are also larger in size (Fig 7c) and appear to have either increased uptake or phagocytic activity, as demonstrated by the retention of Vybrant dye that was initially present in the cytoplasm of the JC CRL 2116 tumor cells (Fig 7d). CD11b expression levels, which are known to be upregulated under certain activation conditions, do not appear to increase under these experimental conditions (Biswas & Sodhi 2002).

Discussion

We present here a relatively simple optical counting setup that brings together several established techniques—including automated microscopy, cellular staining, and cell segmentation—to quantify every cell in an experimental space, without the need for trypsinization or cell scraping. Using whole-well imaging, we demonstrate that taking representative or random images of a well to make a claim about cell viability/counts may be misleading given the non-uniform distribution of cells in a well. In addition, by counting each individual cell using nuclear segmentation, we demonstrate the impressive accuracy and resolution of our optical quantification system. In general, counting single events/cells provides a

298 resolution that cannot be obtained with bulk ensemble measurements, and can significantly
299 improve sensitivity (Chang et al. 2012; Rissin et al. 2010). This approach, in conjunction with
300 whole-well imaging, also offers increased statistical power as the experimentally relevant region
301 is sampled in its entirety.

302 Next, we show that the system can accurately quantify cells up to the confluency limit of
303 the plate. By increasing the surface area of each well however, it is possible to expand the
304 working range of the optical cytometer. Though 12-well plates were used here to accurately
305 quantify up to 100,000 cells/well, it is possible to use 6-well plates or less, with a larger
306 corresponding surface area per well, to push the upper limits of detection.

307 On the lower end of the optical cytometer's operating range, illumination correction,
308 sufficient post-stain washing, and binary quantification make counting of just a single-cell
309 theoretically possible with minimal interference from background or noise. Data from tests that
310 were conducted with only a few cells per well demonstrate the incredible sensitivity of the
311 system, but slight deviations in segmented nuclei-derived counts versus manual counts are
312 evident as demonstrated by the imperfect R^2. While manual counts were performed solely on
313 brightfield images, merging of nuclei in the DAPI channel with cell outlines in the brightfield
314 channel reveal that deviations in the lower range data were actually due to human error.
315 Ultimately, counts obtained via CellProfiler proved more reliable than manual counting
316 validating the ability of the optical cytometer to quantify down to the single-cell level. Systems
317 with improved sensitivity are not only advantageous when conducting screening assays on
318 smaller sized plates (such as 96-, 384-, and 1536-well plates), but also when detecting a very low
319 concentration of cells on large well plates. A sensitive system may also prove useful for
320 detecting rare cell subpopulations in a heterogeneous group (Lin et al. 2011).

Testing of the upper and lower extremes of the optical cytometer reveal the greater than 5-log detection range that can be achieved with the instrument. Systems with a large dynamic range are particularly advantageous for screening cytotoxic compounds such as antineoplastic agents. It has been shown that compounds that reduce cell viability by at least two orders of magnitude *in vitro* are more likely to demonstrate a response in clinical trials, making an assay with an even larger dynamic range more appealing (Frgala et al. 2007). All together, the combination of improved sensitivity, resolution, and dynamic range afforded by the automated optical cytometer opens up the possibility of a new set of cell culture experiments that were not previously feasible.

We next show that certain cytoplasmic and surface stains, in conjunction with a nuclear stain, can be used to effectively differentiate cell populations in a co-culture setup. Vybrant CFDA SE dyes, for example, are designed to form intracellular fluorescent conjugates that homogenously stain the cell cytoplasm, are well-retained, and are not transferred to adjacent cells or passed onto daughter cells during division (Bronner-Fraser 1985; Hodgkin et al. 1996; Lyons & Parish 1994; Nose & Takeichi 1986; Weston & Parish 1990). Alternatively, cells can be stained post-experiment and just prior to imaging using target-specific dyes, such as fluorescently-conjugated antibodies.

For counting of more than one cell type in a co-culture setup, using a mask generated from the fluorescent outlines of either a surface or cytoplasmic stain to delineate which nuclei belong to which cell type proved to be the most robust. To do this, whole-cell fluorescence—generated from either a surface or cytoplasmic stain—is used to create an inclusive mask that retains nuclei contained within. This method can be repeated iteratively for each cell specific stain, eventually grouping every nucleus with its associated cell population. These filtered nuclei

images can then be segmented and quantified using standard nuclear segmentation to generate respective counts for each cell type. This approach is made possible using the unique fluorescent staining and algorithmic combination proposed herein, and overcomes many of the limitations of traditional segmenting systems. A sample workflow of this process with associated images can be found in the supplementary section (Fig S3).

It should be mentioned that many commercial image cytometers largely rely on primary segmentation for the quantification of multiple adherent cell types in a single well. This often requires the utilization of an array of algorithmic functions such as thresholding, contouring, water shedding, cleaning, eroding, dilating, opening, closing, and smoothing to uniquely identify individual cells. Classifiers (both object and pixel) are also occasionally utilized to train systems to recognize user-delineated objects. However, these algorithmic approaches are largely inadequate for quantifying cells with complex morphologies ultimately limiting the accuracy and performance of commercial systems in these settings. For our study in particular, primary segmentation of the cytoplasmic and surface stains alone performed reasonably well when cell morphology was round and staining was homogenous (as was the case with the J774.A1 triple stain). When cell morphology became more spindly (as seen with JC CRL 2116 cells), or staining became more inhomogeneous (as seen with activated J774.A1 cells) however, a marked decrease in primary segmentation performance was observed (data not shown) indicating that the aforementioned algorithmic functions are limited in their generalizability. Using the fluorescent outline of the cell to generate a mask removes the need for primary segmentation of these stains, and instead harnesses the accuracy/power of nuclear segmentation, allowing for highly accurate quantification of multiple cell types with varying morphologies in a co-culture setup. If a user

was already in possession of a commercial optical counting system, the proposed algorithmic approach could be adapted to achieve the same results.

The ability of the optical cytometer to accurately count individual cells of a specific population is best demonstrated by the macrophage-tumor co-culture experiment we recreated. Unfortunately, the use of ^{51}Cr to radiolabel target tumor cells is expensive and manually intensive by today's standards. While cell-permeable fluorogenic protease substrates have been developed as a replacement for ^{51}Cr, neither is capable of dynamically quantifying changes in effector cell (macrophage) count and the tumor cells they target (Packard & Komoriya 2008). A suitable alternative assay to count both tumor cell and macrophage populations does not exist for this particular experiment. Flow cytometry, for example, would not be preferable here because J774.A1 macrophages are not amenable to trypsin treatment, and thus require manual scraping. In addition, standard flow cytometry would struggle to tease out individual counts of each cell type because the data is collected as a relative count to total number of cells gated. As shown in Figure 7b, the quantification of relative counts rather than absolute counts would have led the user to believe that macrophage priming actually promotes tumor cell growth as opposed to inhibiting it (tumor cells represent 18.0% of the total sample in the unprimed control versus 36.1% of the total sample in the LPS + IFNγ primed condition). The optical cell cytometer system we have developed, however, can determine absolute counts of both cell types with remarkable accuracy. With the priming of the J774.A1 macrophages, we were able to not only elucidate the tumoricidal activity of the macrophages, but also the inverse nature of macrophage proliferation and cytotoxic potential.

In addition to cell count, the optical cytometer was able to extract morphological data, such as cell size and mean fluorescence intensity, for every cell. The system is also capable of

extracting additional parametric data, such as cell eccentricity, orientation, number of neighbors, first closest object distance, and granularity, extending its capacity beyond simply counting, and into cytometry. The cytometer is also compatible with other fluorescent-based assay stains including annexin V and/or propidium iodide for assessing cell death, CFSE or BrdU for measuring cell proliferation, and alamarBlue or calcein AM for determining cell viability. For many fields of biology where the interaction between multiple cell types is important, the ability to conduct this type of co-culture experiment may prove invaluable.

Suggestions for improving and expanding the capacities of the optical cell cytometer for co-culture as well as mono-culture studies can be found in the supplementary section. They include recommendations for optimizing workflow, handling of an increasing number of cells/parameters in a single experimental setup (multiplexing), management of multinucleated cells, processing of tissue samples, and analysis of poorly adherent cells. An overview of the technical specifications of the optical cell cytometer can also be found in the supplementary (Additional File 4: Text S1).

Conclusions

All together, the optical cell cytometer is a viable alternative to flow cytometry, and other currently available imaging cytometers, and is available at only a fraction of the cost for labs that already possess a fluorescent microscope. The system is automated and high throughput using tools already available in most labs. Optical cell counting offers unprecedented sensitivity, going down to the single-cell level, while still boasting an impressive dynamic range limited only by the size of the well plate used. Because counts are binary, the system offers remarkable resolution. Further, the use of whole-well images allows for quantification across the entire experimental space conferring remarkable accuracy. In addition to cell counts, other features can

be gathered from each experiment, including the spatial distribution of cells as well as various morphological analyses. The system is also compatible with other fluorescent-based assay stains. Since the system is put together by the user, it is highly customizable, and allows for direct assessment of assay performance.

The optical cytometer has the added benefit of assessing adherent cells directly on the plate without needing to bring them into solution. As a result, the system does not require caustic trypsin treatment to resuspend cells in solution, as is the case with flow cytometry. One of the most promising aspects of the system is that multiple cell types can be plated together and absolute counts of each population can be elucidated. For many fields of biology, absolute counts can help tease out interesting relationships between cell populations that might not be discernible using relative counts. After imaging and analysis, population statistics—including cell counts and fluorescence intensity—can be extracted, thresholded, and displayed in histogram or dot-plot form much like the output of a flow cytometer. Overall, we believe the optical cell cytometer will improve the quality of cell cytometric studies and open up the possibility of a new class of experiments centered around the ability to assess multiple cell types in a co-culture setup. The impressive sensitivity and dynamic range of the instrument are also strongly compelling.

Acknowledgements

We would like to thank the Miller lab for providing the Nikon Eclipse Ti-E inverted fluorescent microscope and the Drezek lab for editorial assistance.

Author's Contributions

Conceived and designed the experiments: VA, RAD. Performed the experiments: YT, AF, AA, BSS, VA. Analyzed the data: VA, YT, AF. Contributed reagents/materials/analysis tools: ALC, RAD. Wrote the paper: VA, PB, ERE, RAD. All authors read and approved the final manuscript.

Conflict of Interest

The authors declare that they have no competing interests

Data Availability

Raw data files can be found at

https://www.dropbox.com/sh/it4e56my94xmlba/AADRuhXlkkX1xnziAu4bYJlLa?dl=0

Funding

No outside funding was received for this project

References

An M, Wijesinghe D, Andreev OA, Reshetnyak YK, and Engelman DM. 2010. pH-(low)-insertion-peptide (pHLIP) translocation of membrane impermeable phalloidin toxin inhibits cancer cell proliferation. *Proc Natl Acad Sci U S A* 107:20246-20250. 10.1073/pnas.1014403107

Arora R, Agarwal S, Mathur SR, Verma K, Iyer VK, and Aron M. 2011. Utility of a limited panel of calretinin and Ber-EP4 immunocytochemistry on cytospin preparation of serous effusions: A cost-effective measure in resource-limited settings. *Cytojournal* 8:14. 10.4103/1742-6413.83233

Arrigoni C, Bersini S, Gilardi M, and Moretti M. 2016. In Vitro Co-Culture Models of Breast Cancer Metastatic Progression towards Bone. *Int J Mol Sci* 17. 10.3390/ijms17091405

Arya H, Kaul Z, Wadhwa R, Taira K, Hirano T, and Kaul SC. 2005. Quantum dots in bio-imaging: Revolution by the small. *Biochem Biophys Res Commun* 329:1173-1177. 10.1016/j.bbrc.2005.02.043

Bastiaens PI, and Squire A. 1999. Fluorescence lifetime imaging microscopy: spatial resolution of biochemical processes in the cell. *Trends Cell Biol* 9:48-52.

Batista U, Garvas M, Nemec M, Schara M, Veranic P, and Koklic T. 2010. Effects of different detachment procedures on viability, nitroxide reduction kinetics and plasma membrane heterogeneity of V-79 cells. *Cell Biol Int* 34:663-668. 10.1042/CBI20090276

Becker W. 2012. Fluorescence lifetime imaging--techniques and applications. *J Microsc* 247:119-136. 10.1111/j.1365-2818.2012.03618.x

Bidarra SJ, Barrias CC, Barbosa MA, Soares R, Amedee J, and Granja PL. 2011. Phenotypic and proliferative modulation of human mesenchymal stem cells via crosstalk with endothelial cells. *Stem Cell Res* 7:186-197. 10.1016/j.scr.2011.05.006

Biswas SK, and Sodhi A. 2002. In vitro activation of murine peritoneal macrophages by monocyte chemoattractant protein-1: upregulation of CD11b, production of proinflammatory cytokines, and the signal transduction pathway. *J Interferon Cytokine Res* 22:527-538. 10.1089/10799900252982007

Brando B, Barnett D, Janossy G, Mandy F, Autran B, Rothe G, Scarpati B, D'Avanzo G, D'Hautcourt JL, Lenkei R, Schmitz G, Kunkl A, Chianese R, Papa S, and Gratama JW. 2000. Cytofluorometric methods for assessing absolute numbers of cell subsets in blood. European Working Group on Clinical Cell Analysis. *Cytometry* 42:327-346.

Bronner-Fraser M. 1985. Alterations in neural crest migration by a monoclonal antibody that affects cell adhesion. *J Cell Biol* 101:610-617.

Bundscherer A, Malsy M, Lange R, Hofmann P, Metterlein T, Graf BM, and Gruber M. 2013. Cell harvesting method influences results of apoptosis analysis by annexin V staining. *Anticancer Res* 33:3201-3204.

Carpenter AE, Jones TR, Lamprecht MR, Clarke C, Kang IH, Friman O, Guertin DA, Chang JH, Lindquist RA, Moffat J, Golland P, and Sabatini DM. 2006. CellProfiler: image analysis software for identifying and quantifying cell phenotypes. *Genome Biol* 7:R100. 10.1186/gb-2006-7-10-r100

Chakrabarti R, Kundu S, Kumar S, and Chakrabarti R. 2000. Vitamin A as an enzyme that catalyzes the reduction of MTT to formazan by vitamin C. *J Cell Biochem* 80:133-138.

Chan GK, Kleinheinz TL, Peterson D, and Moffat JG. 2013. A simple high-content cell cycle assay reveals frequent discrepancies between cell number and ATP and MTS proliferation assays. *PLoS One* 8:e63583. 10.1371/journal.pone.0063583

Chang L, Rissin DM, Fournier DR, Piech T, Patel PP, Wilson DH, and Duffy DC. 2012. Single molecule enzyme-linked immunosorbent assays: theoretical considerations. *J Immunol Methods* 378:102-115. 10.1016/j.jim.2012.02.011

Cooke MJ, Phillips SR, Shah DS, Athey D, Lakey JH, and Przyborski SA. 2008. Enhanced cell attachment using a novel cell culture surface presenting functional domains from extracellular matrix proteins. *Cytotechnology* 56:71-79. 10.1007/s10616-007-9119-7

Cruickshank SM, McVay LD, Baumgart DC, Felsburg PJ, and Carding SR. 2004. Colonic epithelial cell mediated suppression of CD4 T cell activation. *Gut* 53:678-684.

de Goer de Herve MG, Dembele B, Vallee M, Herr F, Cariou A, and Taoufik Y. 2010. Direct CD4 help provision following interaction of memory CD4 and CD8 T cells with distinct antigen-presenting dendritic cells. *J Immunol* 185:1028-1036. 10.4049/jimmunol.0904209

509 Ding M, Chen D, Ma D, Liu P, Song K, Lu H, and Ji Z. 2015. Tuning the Upconversion
510 Luminescence Lifetimes of KYb2 F7 :Ho(3+) Nanocrystals for Optical Multiplexing.
511 *Chemphyschem* 16:3784-3789. 10.1002/cphc.201500795
512 Doak SH, Griffiths SM, Manshian B, Singh N, Williams PM, Brown AP, and Jenkins GJ. 2009.
513 Confounding experimental considerations in nanogenotoxicology. *Mutagenesis*
514 24:285-293. 10.1093/mutage/gep010
515 Espina V, Wulfkuhle JD, Calvert VS, VanMeter A, Zhou W, Coukos G, Geho DH, Petricoin EF,
516 3rd, and Liotta LA. 2006. Laser-capture microdissection. *Nat Protoc* 1:586-603.
517 10.1038/nprot.2006.85
518 Frgala T, Kalous O, Proffitt RT, and Reynolds CP. 2007. A fluorescence microplate
519 cytotoxicity assay with a 4-log dynamic range that identifies synergistic drug
520 combinations. *Mol Cancer Ther* 6:886-897. 10.1158/1535-7163.MCT-04-0331
521 Gedye CA, Hussain A, Paterson J, Smrke A, Saini H, Sirskyj D, Pereira K, Lobo N, Stewart J, Go
522 C, Ho J, Medrano M, Hyatt E, Yuan J, Lauriault S, Meyer M, Kondratyev M, van den
523 Beucken T, Jewett M, Dirks P, Guidos CJ, Danska J, Wang J, Wouters B, Neel B,
524 Rottapel R, and Ailles LE. 2014. Cell surface profiling using high-throughput flow
525 cytometry: a platform for biomarker discovery and analysis of cellular
526 heterogeneity. *PLoS One* 9:e105602. 10.1371/journal.pone.0105602
527 Gerashchenko BI. 2008. Quantitative assessment of cell proliferation in the co-culture of
528 mixed cell populations by flow cytometry. *Cytometry A* 73:492-493.
529 10.1002/cyto.a.20546
530 Gerashchenko BI, and Howell RW. 2013. Flow cytometry-based quantification of cell
531 proliferation in the mixed cell co-culture. *Curr Protoc Cytom* Chapter 9:Unit9 40.
532 10.1002/0471142956.cy0940s63
533 Goers L, Freemont P, and Polizzi KM. 2014. Co-culture systems and technologies: taking
534 synthetic biology to the next level. *J R Soc Interface* 11. 10.1098/rsif.2014.0065
535 Gross HJ, Verwer B, Houck D, Hoffman RA, and Recktenwald D. 1995. Model study detecting
536 breast cancer cells in peripheral blood mononuclear cells at frequencies as low as
537 10(-7). *Proc Natl Acad Sci U S A* 92:537-541.
538 Hamid R, Rotshteyn Y, Rabadi L, Parikh R, and Bullock P. 2004. Comparison of alamar blue
539 and MTT assays for high through-put screening. *Toxicol In Vitro* 18:703-710.
540 10.1016/j.tiv.2004.03.012
541 Hodgkin PD, Lee JH, and Lyons AB. 1996. B cell differentiation and isotype switching is
542 related to division cycle number. *J Exp Med* 184:277-281.
543 Holt DJ, Chamberlain LM, and Grainger DW. 2010. Cell-cell signaling in co-cultures of
544 macrophages and fibroblasts. *Biomaterials* 31:9382-9394.
545 10.1016/j.biomaterials.2010.07.101
546 Jones TR, Carpenter A, and Golland P. 2005. Voronoi-Based Segmentation of Cells on Image
547 Manifolds. In: Liu Y, Jiang T, and Zhang C, eds. *Computer Vision for Biomedical Image*
548 *Applications: First International Workshop, CVBIA 2005, Beijing, China, October 21,*
549 *2005 Proceedings*. Berlin, Heidelberg: Springer Berlin Heidelberg, 535-543.
550 Katt ME, Placone AL, Wong AD, Xu ZS, and Searson PC. 2016. In Vitro Tumor Models:
551 Advantages, Disadvantages, Variables, and Selecting the Right Platform. *Front*
552 *Bioeng Biotechnol* 4:12. 10.3389/fbioe.2016.00012
553 Koh CM. 2013. Preparation of cells for microscopy using cytospin. *Methods Enzymol*
554 533:235-240. 10.1016/B978-0-12-420067-8.00016-7

555 Krajcovic M, Johnson NB, Sun Q, Normand G, Hoover N, Yao E, Richardson AL, King RW,
556 Cibas ES, Schnitt SJ, Brugge JS, and Overholtzer M. 2011. A non-genetic route to
557 aneuploidy in human cancers. *Nat Cell Biol* 13:324-330. 10.1038/ncb2174
558 Lee-Montiel FT, Li P, and Imoukhuede PI. 2015. Quantum dot multiplexing for the profiling
559 of cellular receptors. *Nanoscale* 7:18504-18514. 10.1039/c5nr01455g
560 Lin Y, Trouillon R, Safina G, and Ewing AG. 2011. Chemical analysis of single cells. *Anal*
561 *Chem* 83:4369-4392. 10.1021/ac2009838
562 Lyons AB, and Parish CR. 1994. Determination of lymphocyte division by flow cytometry. *J*
563 *Immunol Methods* 171:131-137.
564 Mazia D, Schatten G, and Sale W. 1975. Adhesion of cells to surfaces coated with polylysine.
565 Applications to electron microscopy. *J Cell Biol* 66:198-200.
566 Michalet X, Pinaud FF, Bentolila LA, Tsay JM, Doose S, Li JJ, Sundaresan G, Wu AM, Gambhir
567 SS, and Weiss S. 2005. Quantum dots for live cells, in vivo imaging, and diagnostics.
568 *Science* 307:538-544. 10.1126/science.1104274
569 Miki Y, Ono K, Hata S, Suzuki T, Kumamoto H, and Sasano H. 2012. The advantages of co-
570 culture over mono cell culture in simulating in vivo environment. *J Steroid Biochem*
571 *Mol Biol* 131:68-75. 10.1016/j.jsbmb.2011.12.004
572 Nasi M, De Biasi S, Bianchini E, Gibellini L, Pinti M, Scacchetti T, Trenti T, Borghi V, Mussini
573 C, and Cossarizza A. 2015. Reliable and accurate CD4+ T cell count and percent by
574 the portable flow cytometer CyFlow MiniPOC and "CD4 Easy Count Kit-Dry", as
575 revealed by the comparison with the gold standard dual platform technology. *PLoS*
576 *One* 10:e0116848. 10.1371/journal.pone.0116848
577 Nose A, and Takeichi M. 1986. A novel cadherin cell adhesion molecule: its expression
578 patterns associated with implantation and organogenesis of mouse embryos. *J Cell*
579 *Biol* 103:2649-2658.
580 Novotney M, Chang ZL, Uchiyama H, and Suzuki T. 1991. Protein kinase C in tumoricidal
581 activation of mouse macrophage cell lines. *Biochemistry* 30:5597-5604.
582 Packard BZ, and Komoriya A. 2008. Intracellular protease activation in apoptosis and cell-
583 mediated cytotoxicity characterized by cell-permeable fluorogenic protease
584 substrates. *Cell Res* 18:238-247. 10.1038/cr.2008.17
585 Pappas D, and ebrary Inc. 2010. Practical cell analysis. Hoboken, N.J.: Wiley,. p xx, 294 p.
586 Pinaud F, Michalet X, Bentolila LA, Tsay JM, Doose S, Li JJ, Iyer G, and Weiss S. 2006.
587 Advances in fluorescence imaging with quantum dot bio-probes. *Biomaterials*
588 27:1679-1687. 10.1016/j.biomaterials.2005.11.018
589 Quent VM, Loessner D, Friis T, Reichert JC, and Hutmacher DW. 2010. Discrepancies
590 between metabolic activity and DNA content as tool to assess cell proliferation in
591 cancer research. *J Cell Mol Med* 14:1003-1013. 10.1111/j.1582-4934.2010.01013.x
592 Rissin DM, Kan CW, Campbell TG, Howes SC, Fournier DR, Song L, Piech T, Patel PP, Chang
593 L, Rivnak AJ, Ferrell EP, Randall JD, Provuncher GK, Walt DR, and Duffy DC. 2010.
594 Single-molecule enzyme-linked immunosorbent assay detects serum proteins at
595 subfemtomolar concentrations. *Nat Biotechnol* 28:595-599. 10.1038/nbt.1641
596 Schoenborn JR, and Wilson CB. 2007. Regulation of interferon-gamma during innate and
597 adaptive immune responses. *Adv Immunol* 96:41-101. 10.1016/S0065-
598 2776(07)96002-2
599 Sklar LA. 2005. *Flow cytometry for biotechnology*. New York: Oxford University Press.

600 Sternberg SR. 1983. Biomedical Image Processing. *Computer* 16:22-34.
601 10.1109/MC.1983.1654163
602 Suzuki S, Sato M, Senoo H, and Ishikawa K. 2004. Direct cell-cell interaction enhances pro-
603 MMP-2 production and activation in co-culture of laryngeal cancer cells and
604 fibroblasts: involvement of EMMPRIN and MT1-MMP. *Exp Cell Res* 293:259-266.
605 Trotta E, Del Grosso N, Erba M, Melino S, Cicero D, and Paci M. 2003. Interaction of DAPI
606 with individual strands of trinucleotide repeats. Effects of replication in vitro of the
607 AAT x ATT triplet. *Eur J Biochem* 270:4755-4761.
608 Ulukaya E, Colakogullari M, and Wood EJ. 2004. Interference by anti-cancer
609 chemotherapeutic agents in the MTT-tumor chemosensitivity assay. *Chemotherapy*
610 50:43-50. 10.1159/000077285
611 Vincent L, and Soille P. 1991. Watersheds in digital spaces: an efficient algorithm based on
612 immersion simulations. *IEEE Transactions on Pattern Analysis and Machine*
613 *Intelligence* 13:583-598. 10.1109/34.87344
614 Vistica DT, Skehan P, Scudiero D, Monks A, Pittman A, and Boyd MR. 1991. Tetrazolium-
615 based assays for cellular viability: a critical examination of selected parameters
616 affecting formazan production. *Cancer Res* 51:2515-2520.
617 Weihua Z, Lin Q, Ramoth AJ, Fan D, and Fidler IJ. 2011. Formation of solid tumors by a
618 single multinucleated cancer cell. *Cancer* 117:4092-4099. 10.1002/cncr.26021
619 Wen H, Cui Q, Meng H, Lai F, Wang S, Zhang X, Chen X, Cui H, and Yin D. 2016. A high-
620 resolution method to assess cell multinucleation with cytoplasm-localized
621 fluorescent probes. *Analyst* 141:4010-4013. 10.1039/c6an00613b
622 Weston SA, and Parish CR. 1990. New fluorescent dyes for lymphocyte migration studies.
623 Analysis by flow cytometry and fluorescence microscopy. *J Immunol Methods*
624 133:87-97.
625

626

627

628

629

Figure 1(on next page)

Workflow schematic.

Using tools available in most labs, we have created a relatively simple optical counting setup for the quantification of multiple adherent cell types in a multiwell plate. After plating cells, adding condition, and fluorescent staining, the proposed system uses a standard fluorescent microscope to capture whole-well images. Image data is then run through ImageJ for preprocessing and CellProfiler for analysis to generate both absolute cell counts for every well as well as morphological values. Furthermore, utilizing a combination of staining techniques, multiple cell types in a co-culture setup (Cell A & B as an example) can be uniquely identified and absolutely counted.

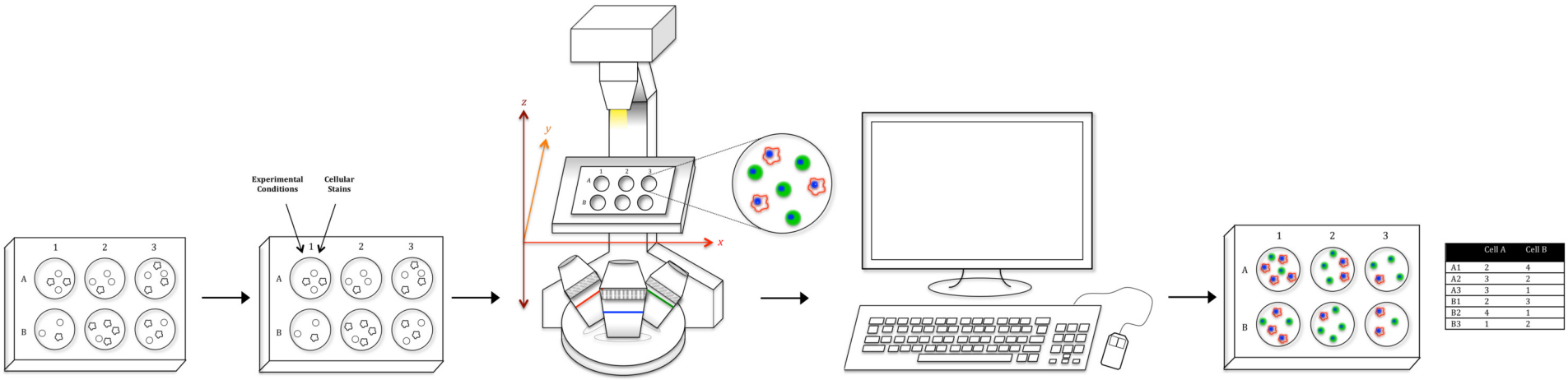

	Cell A	Cell B
A1	2	4
A2	3	2
A3	3	1
B1	2	3
B2	4	1
B3	1	2

PeerJ Preprints | https://doi.org/10.7287/peerj.preprints.26584v1 | CC BY 4.0 Open Access | rec: 1 Mar 2018, publ: 1 Mar 2018

Figure 2(on next page)

Automated, whole-well imaging.

Using a fluorescent microscope with motorized x, y, and z stage, images spanning the entire well can be sequentially captured and stitched together to produce a high resolution, whole-well image. In the image series above, cell nuclei stained with DAPI were imaged on a 48-well plate with a 10x objective and stitched together. Sequential zooms of the whole-well image demonstrate the incredibly high resolution of the photo, which enables single-cell counting and analysis using a cell segmentation software like CellProfiler (used to generate the final mask).

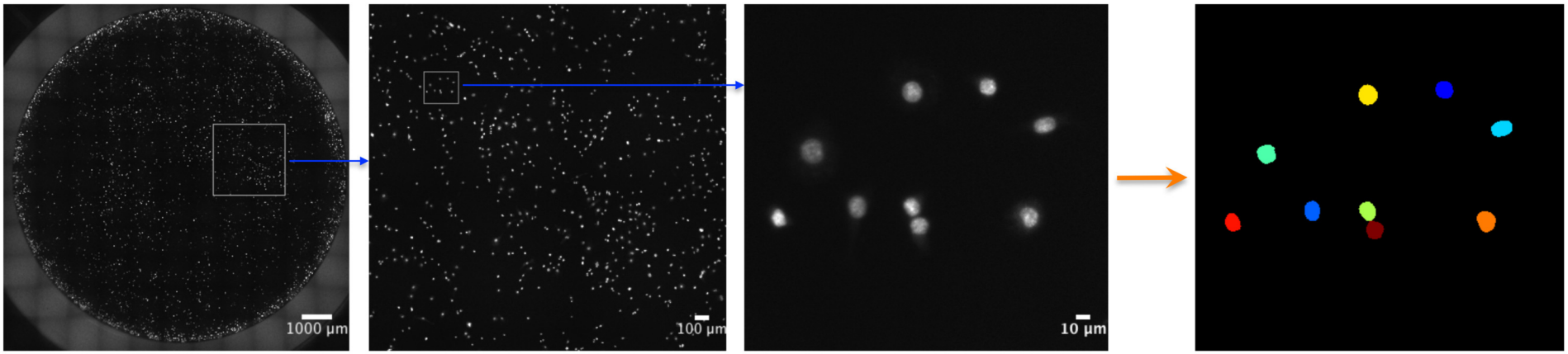

PeerJ Preprints | https://doi.org/10.7287/peerj.preprints.26584v1 | CC BY 4.0 Open Access | rec: 1 Mar 2018, publ: 1 Mar 2018

Figure 3(on next page)

Power of whole-well imaging and nuclear quantification.

A linear dilution series of JC CRL 2116 cells going from 10,000 cells/well down to 1,000 cells/well was plated on a 48-well plate. Whole-well images of cell nuclei stained with DAPI were then captured and processed to produce either (a) five random images, (b) box crop, or (c) whole-well images, which were then used to determine cell count and generate a linear curve. Accuracy improves significantly as the percent of the experimental space being assayed increases. Error bars represent the standard deviation between triplicate conditions.

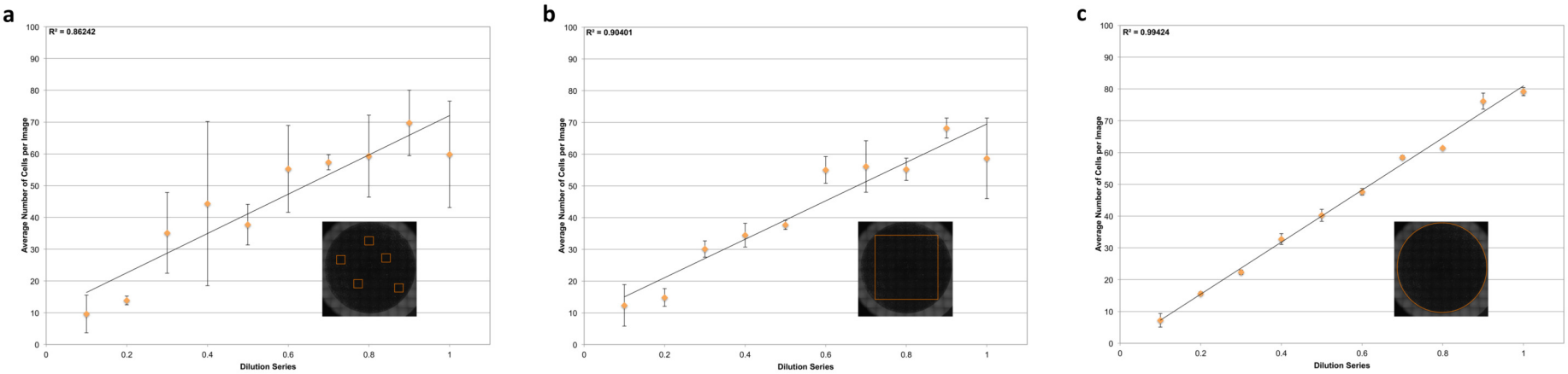

Figure 4(on next page)

Determining dynamic range.

Half-log dilutions of JC CRL 2116 cells going from 100,000 cells/well down to 100 cells/well were plated on a 12-well plate (an experiment spanning three orders of magnitude). Cell nuclei stained with DAPI were then quantified and used to generate a linear curve. The system performs robustly over a wide dynamic range and is limited only by the surface area of the multiwell. Error bars represent the standard deviation between triplicate conditions.

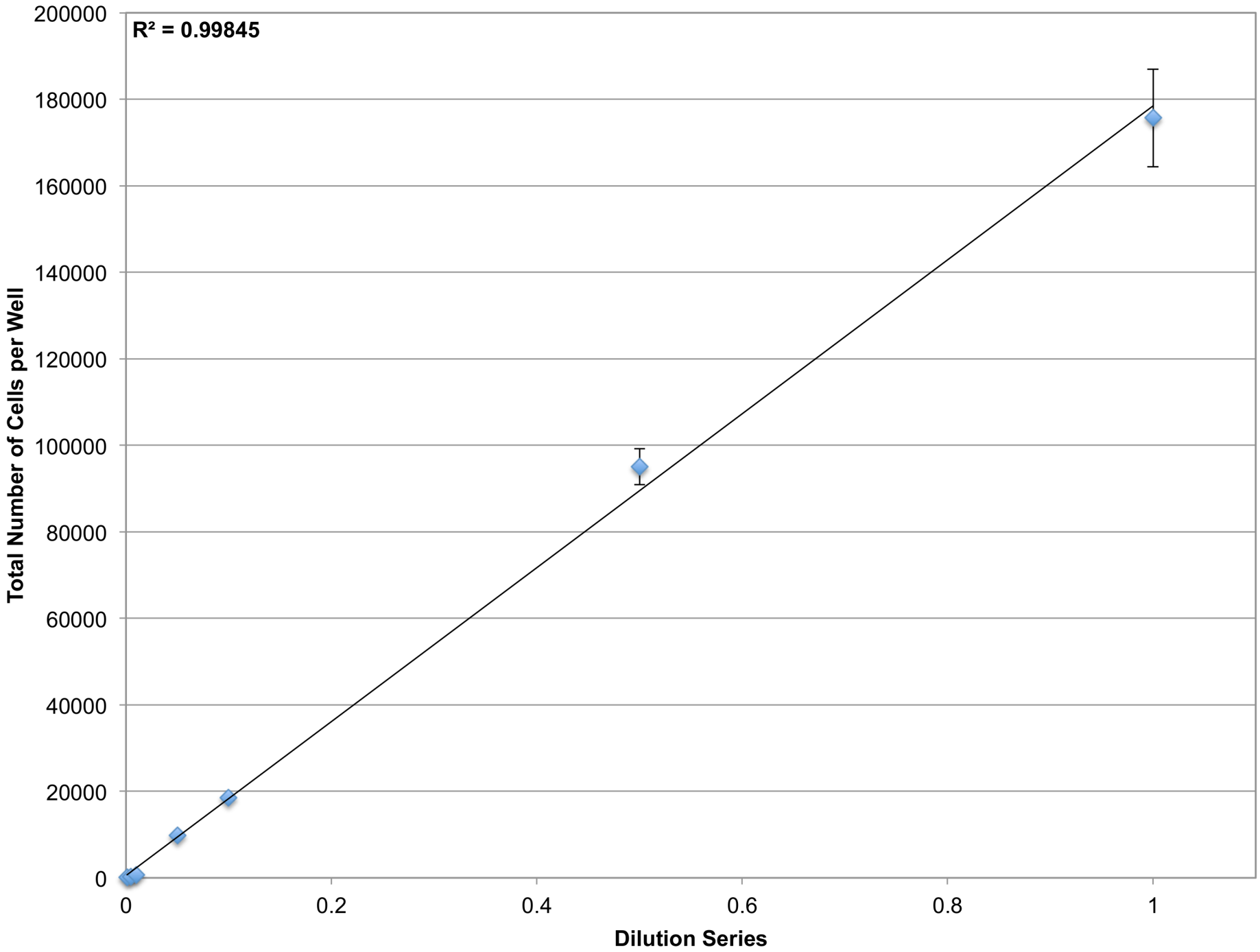

PeerJ Preprints | https://doi.org/10.7287/peerj.preprints.26584v1 | CC BY 4.0 Open Access | rec: 1 Mar 2018, publ: 1 Mar 2018

Figure 5(on next page)

Establishing sensitivity.

Various concentrations of JC CRL 2116 cells going from 100 cells/well down to 1 cell/well were plated on a 48-well plate. CellProfiler-derived counts of DAPI stained nuclei were compared with cell counts obtained by human assessment of associated brightfield images for each well. The system performs robustly even at the single-cell level with most deviations attributable to human error when manually counting.

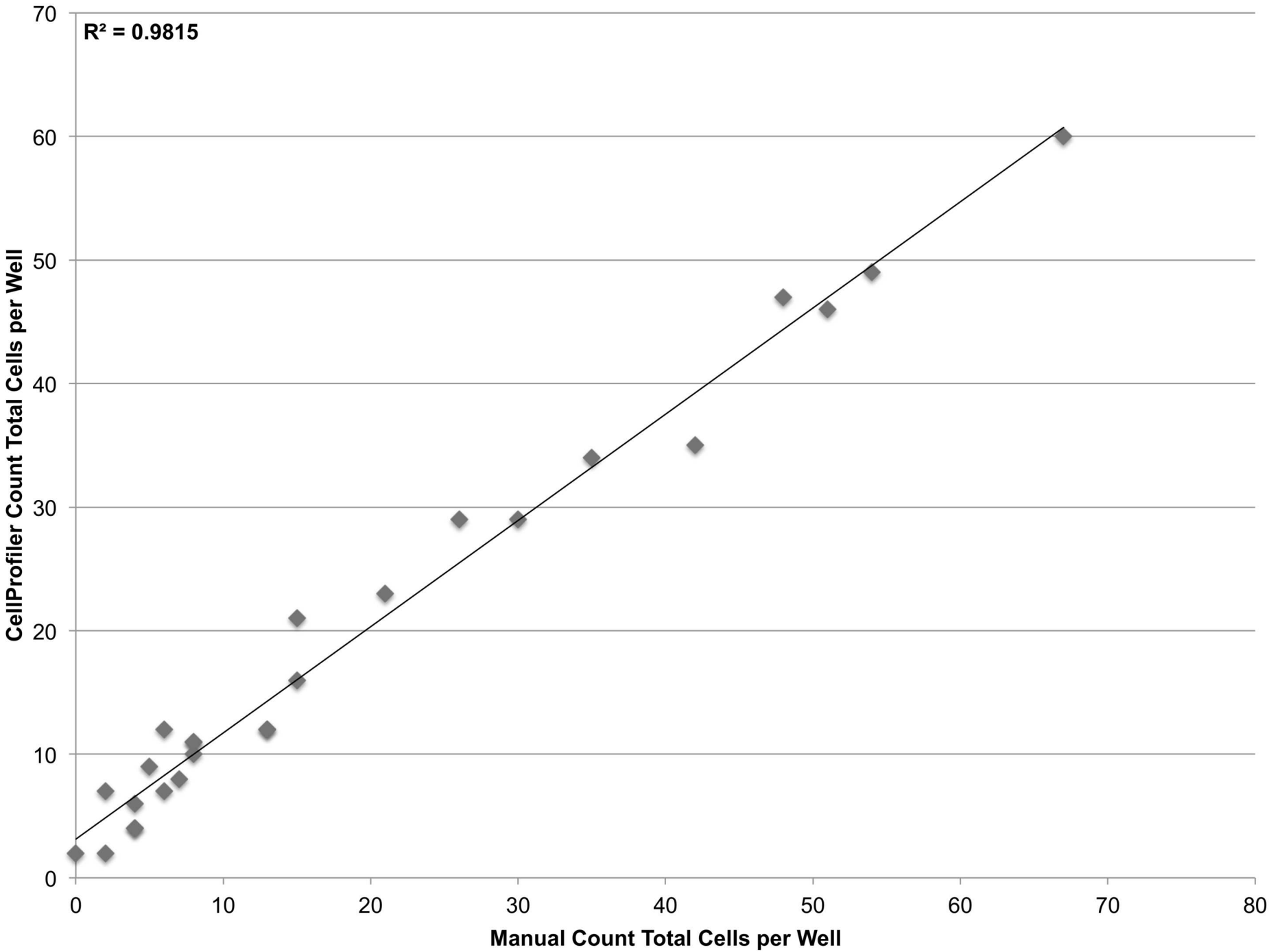

PeerJ Preprints | https://doi.org/10.7287/peerj.preprints.26584v1 | CC BY 4.0 Open Access | rec: 1 Mar 2018, publ: 1 Mar 2018

Figure 6(on next page)

Secondary quantification of surface and cytoplasmic stains using nuclei as seeds.

A linear dilution series of J774.A1 cells going from 10,000 cells/well down to 1,000 cells/well was plated on a 48-well plate. Cells were stained with Vybrant CFDA SE (cytoplasmic stain), phycoerythrin (PE)-conjugated anti-CD11b antibodies (surface stain), and DAPI (nuclear stain). Using nuclei as seeds, cells delineated by a surface or cytoplasmic stain could be accurately quantified as demonstrated by the near-perfect R^2. Error bars represent the standard deviation between triplicate conditions.

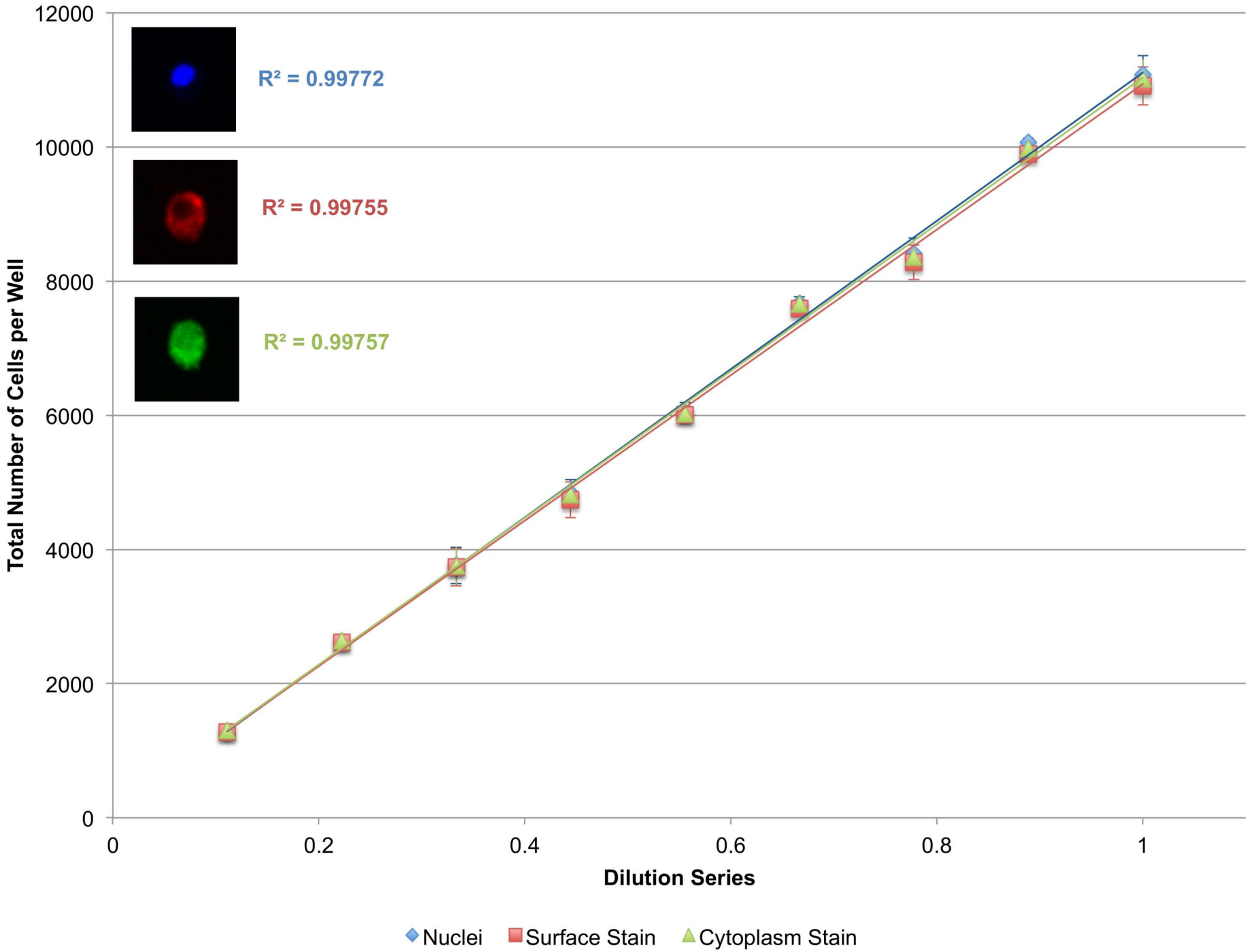

PeerJ Preprints | https://doi.org/10.7287/peerj.preprints.26584v1 | CC BY 4.0 Open Access | rec: 1 Mar 2018, publ: 1 Mar 2018

Figure 7 (on next page)

Tumoricidal properties of primed macrophages in the presence of co-cultured tumor cells.

J774.A1 macrophages were primed with either IFNγ, LPS, or both and subsequently co-cultured with JC CRL 2116 tumor cells. J774.A1 cells were labeled with PE-conjugated anti-CD11b antibodies (red surface stain) while JC CRL 2116 cells were labeled with Vybrant (green cytoplasmic stain). Both cells were also stained with DAPI. (a) Normalized and (b) absolute cell counts as well as (c) cell area were determined for each condition. (d) CD11b expression levels as well as macrophage uptake/phagocytic activity were calculated by extracting the mean fluorescent intensity of macrophage PE and Vybrant staining respectively. The experiment reveals an interesting, dynamic relationship between activated macrophages and target tumor cells that would have been missed by any setup that looks at relative counts. Data for (a), (c), and (d) are normalized to the unprimed control. Error bars represent the standard deviation between triplicate conditions.